NOTES 12(a)

ANNULAR PRESSURE SEALS

Summary

Annular (damper) seals restrict secondary leakage between stages in a centrifugal pump or compressor . The lecture details the physical principle for generation of a direct stiffness in annular damper seals. Seals also generate force coefficients, stiffness-damping-inertia, that greatly affect the rotordynamics of pumps, in particular those handling large density fluids. Highlights on the bulk-flow analysis of annular seals are given with details on the performance of two water seals – long and short, featuring the advantages of an anti-swirl brake to enhance the seal rotordynamic stability.

Background

Seal rotordynamic characteristic have a primary influence on the stability response of high-performance turbomachinery [1]. Non-contacting fluid seals, as shown in Figure 1, are leakage control devices minimizing secondary flows in pumps and compressors. The working fluid is a process liquid of light viscosity or a process gas. Annular seals, although geometrically similar to plain journal bearings, have a different flow structure dominated by flow turbulence and fluid inertia effects. Operating characteristics unique to seals are the large axial pressure gradients and large clearance to radius ratios, while the axial development of the circumferential velocity is of importance in the generation of cross-coupled (hydrodynamic) forces. Textured stator surfaces (macro roughness) to reduce the impact of undesirable cross-coupled dynamic forces and improve seal stability are by now common practice in damper seal technology [2]. Furthermore, annular seals as Lomakin bearings have potential application as support elements (damping bearings) in high speed cryogenic turbo pumps as well in process gas applications (compressors) [3].

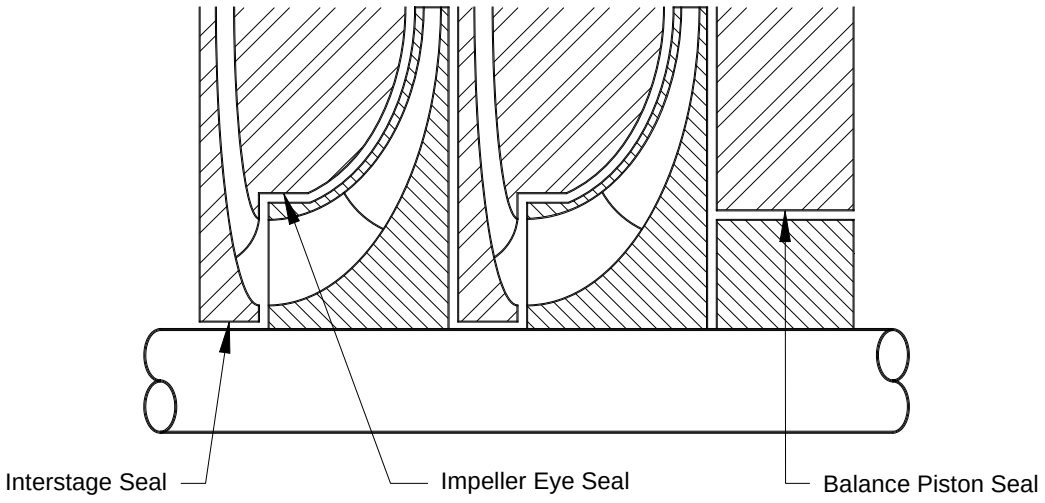

Figure 1: Seals in a Multistage Centrifugal Pump or Compressor

The importance of seal flow phenomenon and its influence on the dynamic response of actual turbomachinery have prompted a large number of theoretical and experimental investigations. Seals, due to their relative position within the rotor-bearing system, can modify sensibly the system dynamic behavior since these elements typically "see" large amplitude rotor motions. This assertion is of particular importance in back-to-back compressor arrangements (see Figure 2). Furthermore, the force coefficients – stiffness, damping and inertia- of annular seals in large density liquid pumps can be as large as those arising in the oil-lubricated bearings; thus the seal elements effectively become load paths and modify the pump rotordynamic behavior. “Wet” and “dry” critical speeds, i.e. those accounting for seals’ forces and not, can be markedly different as noted in [1, 4].

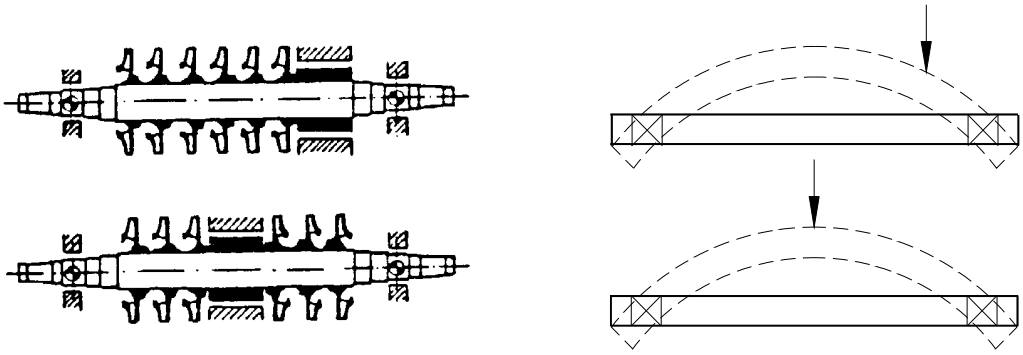

Figure 2: Straight-Through and Back-to-back Compressor Configurations and 1st Mode Shapes (Childs [1])

Black [5] first explained the influence of seal forces on the rotordynamic behaviour of pumps. Since 1980, Childs and co-workers at TAMU conducted a comprehensive program for the analysis and testing of the dynamic force response of liquid and gas annular seals. Experimental programs with damper seals featuring various stator surface machined textures (macro roughness), see Figure 3, have confirmed the benefit of higher net damping forces and less leakage than in smooth surface seals. Reference [2] details major developments in gas seal applications, for example.

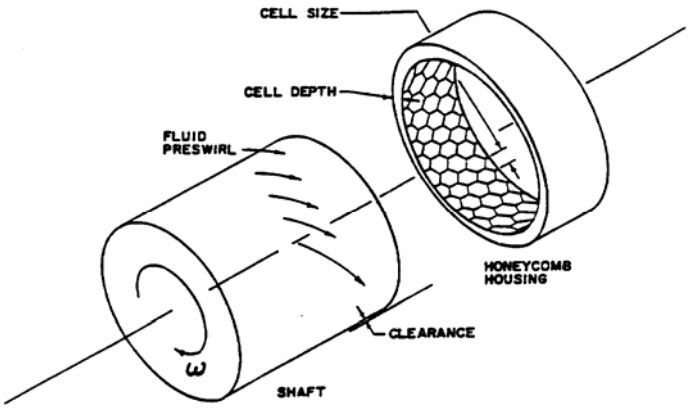

Figure 3: Honeycomb seal for liquid turbopump (Childs [1])

This lecture notes presents:

a) The physical mechanism by which a direct stiffness arises in annular pressure seals even without journal (shaft) rotation. The model analyzes the flow balance and pressure drops at the entrance of a channel and on the ensuing thin film land. A maximum (optimum) stiffness is then predicted for a certain flow resistance balance between the entrance and land pressure drops.
b) A brief description of the bulk-flow equations for prediction of the flow and force coefficients in annular pressure seals.
c) Discussion of predictions for two water seals, long and short, for application as neck ring and interstage seals. The influences of seal length and inlet swirl on the rotordynamic force coefficients are thoroughly discussed.

Refer to Childs [1] and San Andrés [6] for a critical review of the archival literature related to the chronological developments in annular pressure seal analyses as well as experimental results validating the model predictions.

This lecture content material does not include a discussion on labyrinth seals or deep groove seals for liquid pump applications. Labyrinth seals are more common in centrifugal compressors.

Non-contacting face seal technology has reached great maturity for specialized pumps handling chemically harmful fluids. This type of sealing system is not presented here, see Ref. [7] for details.

Generation of stiffness in a sudden film contraction [8]

Figure 4 shows the typical geometry of an annular pressure seal. Fluid at a high pressure (P_s) flows through an annular gap of radial clearance (c) and discharges at the exit pressure (P_a). L and D represent the seal length and diameter, respectively.

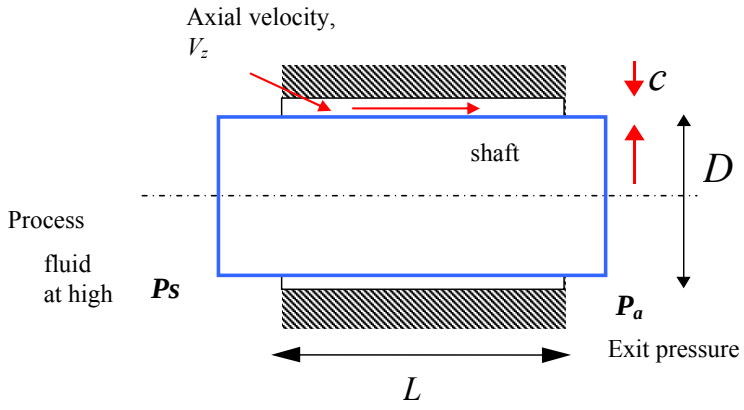

Figure 4: Geometry of an annular pressure seal

The principle by which a direct stiffness originates in an annular seal is due to the inertial pressure drop at the seal inlet plane and its close interaction with the pressure drop (and

flow resistance) within the seal film land. The entrance effect is solely due to fluid inertia accelerating the fluid from an upstream stagnant condition to a flow with high axial speed and reduced static pressure at the seal inlet. The effect is known as **Lomakin**, in honor of the named Russian engineer who discovered the phenomenon in the late 1950's.

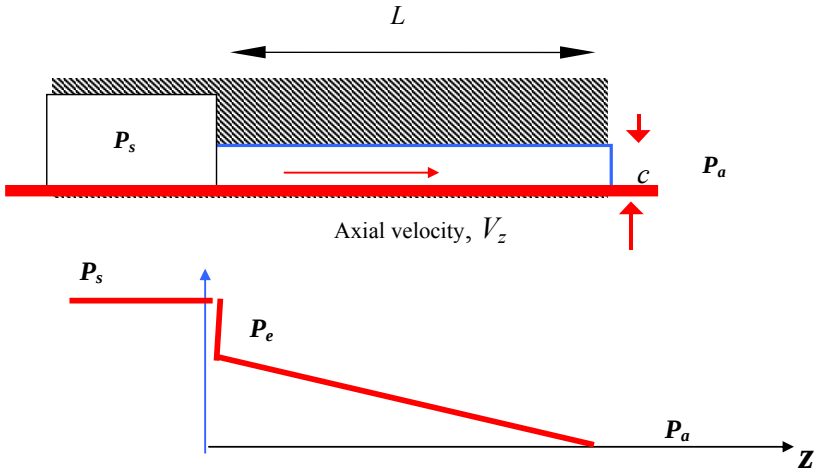

Figure 5: Sudden pressure drop due to fluid inertia in a sudden contraction

In the following, the sealing fluid is regarded as incompressible and isoviscous and the turbulent flow through the film land fully developed. A similar analysis, though more laborious, can be conducted for compressible fluids (gases). Incidentally, laminar flow conditions may be easily accounted for in the following development [6].

Consider the flow through a channel of height c and length L, as shown in Figure 5. The channel is infinitely long in the direction perpendicular to the plane of the page. The fluid flows from a large plenum at pressure P_s, and as it enters the seal, there is a sudden pressure drop (and flow acceleration) at the sudden contraction. This Bernoulli-like effect is solely due to fluid inertia and expressed by,

$$P_e = P_s - \frac{1}{2}\rho(1+\xi)V_z^2 \qquad (1)$$

where P_e is the fluid entrance pressure at the seal inlet, V_z is the bulk-flow axial velocity, and ξ is a non-isentropic (empirical) entrance loss coefficient (typical value ranging from 0.0 to 0.25). In equation (1), fluid stagnant conditions are considered well upstream of the seal inlet plane. Within the seal of land length L and small film clearance *(c),* a linear pressure drop evolves due to viscous (turbulent flow) effects, i.e.

$$P_e - P_a = +\frac{\mu\ k_z}{c^2} V_z L \qquad (2)$$

where $\kappa_z = 12$ for laminar flow or $\kappa_z = f_z R_a$ for turbulent flow. Note that the axial velocity is constant along the thin film due to flow continuity, i.e. $V_z \cdot c = Q_z$. In turbulent flows, the shear parameter κ_z is a function of the axial flow Reynolds number (R_a). Using Hirs' formulation [9],

$$k_z = f_z\, R_a = (n\, R_a^m)\, R_a = n\, R_a^{m+1} \quad ; \quad R_a = \frac{\rho\, V_z\, c}{\mu} \tag{3}$$

with n = 0.0066, m = -0.25 for smooth surface conditions. Thus, for turbulent flows, equation (2) becomes

$$P_e - P_a = \rho \frac{V_z^2\, L}{c}\, f_z \tag{4}$$

Combining equations (1) and (4) renders the axial velocity V_z, *i.e.*

$$V_z^2 = \frac{P_s - P_a}{\frac{\rho}{2}(1 + \zeta) + \rho \frac{L}{c}\, f_z} \tag{5}$$

The procedure is iterative since the friction factor (f_z) is a function of the axial velocity (V_z). Note that $\frac{\rho}{2}(1+\zeta)$ *and* $\rho \frac{L}{c} f_z$ can be thought as **fluidic resistances** [8]. The flow rate per unit depth (or seal circumference) is $Q_z = V_z \cdot c$. Thus, an increase in entrance loss factor as well as large friction in the land and seal length produce a reduction in leakage. The entrance pressure is also determined from equations (4) and (5) as

$$P_e - P_a = \frac{P_s - P_a}{\left\{1 + \frac{(1+\zeta)}{2 f_z} \frac{c}{L}\right\}} \tag{6}$$

Note that the larger the ratio, $[\frac{(1+\zeta)}{2 f_z} \frac{c}{L}]$, the larger the entrance pressure drop $(P_s - P_e)$.

Consider a small variation in film thickness so that $c = c_o - \Delta c$, with $\Delta c << c$. A positive value of Δc means a reduction in the local film thickness. The axial velocity and entrance pressure also undergo small changes, i.e.

$$V_z = V_{zo} + \Delta V_z; \quad P_e = P_{eo} + \Delta P \tag{7}$$

A perturbation analysis of all variables, including the friction factors, leads to.

$$\Delta V_z = \frac{-\Delta P}{\rho (1 + \zeta)\, V_{zo}}; \quad \Delta P = \frac{(P_{eo} - P_a)(1 - m)}{1 + \frac{(m+2)(P_{eo} - P_a)}{2(P_s - P_{eo})}} \frac{\Delta c}{c_o} \tag{8}$$

If ΔP is positive, then ΔV_z is negative, *i.e.* when the film thickness decreases ($-\Delta c < 0$) and ΔP raises, this produces a reduction in axial velocity V_z.

Integration of the pressure field over the channel length (L) and depth (B) produces a fluid film reaction force (F)

$$F = B \int_0^L (P - P_a)\, dz = (P_e - P_a) B \frac{L}{2} = F_o + K\, \Delta c \tag{9}$$

The seal static stiffness (K) equals

$$K = \frac{(p_{eo})(1-m)}{1 + \frac{(m+2)(p_{eo})}{2(1-p_{eo})}} \frac{BL}{2c_o}(P_s - P_a) \qquad (10)$$

where $p_{eo} = \frac{P_{eo} - P_a}{P_s - P_a}$ is an entrance pressure ratio. A dimensionless stiffness follows as:

$$\overline{K} = \frac{K}{\frac{BL}{2c_o}(P_s - P_a)} = \frac{(p_{eo})(1-m)}{1 + \frac{(m+2)(p_{eo})}{2(1-p_{eo})}} \qquad (11)$$

For smooth surfaces (m=-0.25). At p_{eo}=0.515 the stiffness is a maximum, $\overline{K}_{max}$=0.3336. That is, an optimum stiffness arises when the inertial entrance pressure drop is slightly larger than 50% of the available pressure drop (P_s-P_a) across the channel length (L). Figure 6 displays the stiffness as a function of the entrance pressure ratio (p_{eo}). Small values of p_{eo} ($\rightarrow$0) indicate too large entrance pressure losses due to fluid inertia, while too large values of p_{eo} ($\rightarrow$1) show too much fluid resistance through the channel length (film land with tight clearance or overly long). None of these two conditions are favorable to induce a pronounced stiffening effect in an annular pressure seal.

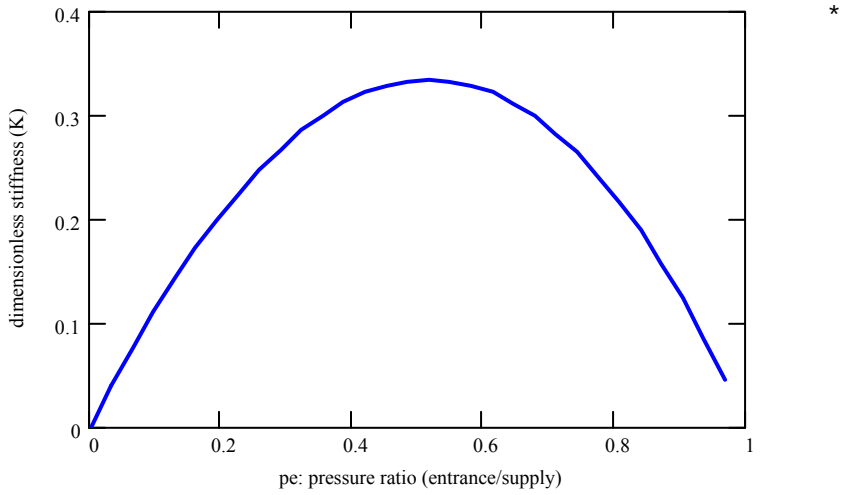

Figure 6: Dimensionless stiffness versus entrance pressure ratio in a thin channel with a sudden inlet contraction

Turbulent bulk flow model in annular pressure seals

Most annular pressure seal analyses predict the dynamic force coefficients due to rotor axis translations about an equilibrium point, i.e. for cylindrical whirl motions. Dynamic force and moment coefficients due to rotor axis angular displacements are of importance in long annular seals, in particular balance pistons and in submerged pump motors [10].

Figure 7 shows the four degrees of freedom in a long annular seal. For small amplitude shaft translational motions $\Delta e_X(t)$, $\Delta e_Y(t)$ along two perpendicular axes (X,Y), and rotations $\delta_X(t)$, $\delta_Y(t)$ around these axes, the seal reaction forces (F_X ,F_Y) and yawing and pitching moments (M_X, M_Y) can be characterized by the following equation:

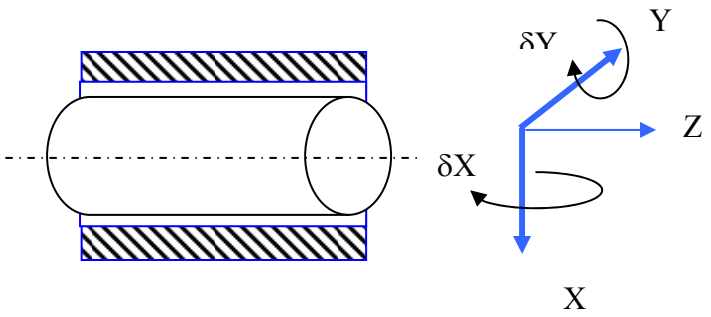

Figure 7: Seal with rotor translations (X,Y) and angulations (δX, δY)

$$\begin{bmatrix} F_X \\ F_Y \\ M_X \\ M_Y \end{bmatrix} = -\begin{bmatrix} K_{XX} & K_{XY} & K_{X\delta X} & K_{X\delta Y} \\ K_{YX} & K_{XX} & K_{X\delta Y} & K_{X\delta X} \\ K_{\delta XX} & K_{\delta XY} & K_{\delta X\delta X} & K_{\delta X\delta Y} \\ -K_{\delta XY} & K_{\delta XX} & K_{\delta X\delta Y} & K_{\delta X\delta X} \end{bmatrix} \begin{bmatrix} \Delta e_X \\ \Delta e_Y \\ \delta_X \\ \delta_Y \end{bmatrix}$$

$$-\begin{bmatrix} C_{XX} & C_{XY} & C_{X\delta X} & C_{X\delta Y} \\ C_{YX} & C_{XX} & C_{X\delta Y} & C_{X\delta X} \\ C_{\delta XX} & C_{\delta XY} & C_{\delta X\delta X} & C_{\delta X\delta Y} \\ C_{\delta XY} & C_{\delta XX} & C_{\delta X\delta Y} & C_{\delta X\delta X} \end{bmatrix} \begin{bmatrix} \Delta \dot{e}_X \\ \Delta \dot{e}_Y \\ \delta_{\dot{X}} \\ \delta_{\dot{Y}} \end{bmatrix}$$

$$-\begin{bmatrix} M_{XX} & M_{XY} & M_{X\delta X} & M_{X\delta Y} \\ M_{YX} & M_{XX} & M_{X\delta Y} & M_{X\delta X} \\ M_{\delta XX} & M_{\delta XY} & M_{\delta X\delta X} & M_{\delta X\delta Y} \\ M_{\delta XY} & M_{\delta XX} & M_{\delta X\delta Y} & M_{\delta X\delta X} \end{bmatrix} \begin{bmatrix} \Delta \ddot{e}_X \\ \Delta \ddot{e}_Y \\ \delta_{\ddot{X}} \\ \delta_{\ddot{Y}} \end{bmatrix} \qquad (12)$$

Equation (12) shows the complexity of a seal dynamic forced performance. There are 16 stiffness coefficients, 16 damping coefficients, and 16 added mass or fluid inertia coefficients. Most rotordynamic software analyses consider only the 4 stiffness, 4 damping and 4 inertia force coefficients due to shaft lateral motions *(X, Y)*[1].

In an annular seal, the flow regime is characterized by high levels of flow turbulence due to the large axial pressure drop $(P_s - P_a)$ and high surface speed (ΩR) of the rotating shaft. A sudden pressure loss and fluid acceleration occur at the seal inlet plane due to the local contraction from the upstream plenum into the film clearance. The smallness of the seal clearance *(c)* as compared to its length or diameter $(L, \pi D)$ allows cross-film integration of the three dimensional momentum and continuity equations, thus rendering a simpler set of transport equations for the bulk-flow velocities (V_x, V_z) and pressure *(P)* field [1, 6, 10].

[1] XLTRC[2] rotordynamics software suite at Texas A&M University does consider the full set of seal force and moment coefficients.

The bulk-flow equations for fully developed turbulent flows at high Reynolds numbers are given by [6]:

$$\frac{\partial}{\partial x}\left(hV_x\right)+\frac{\partial}{\partial z}\left(hV_z\right)+\frac{\partial h}{\partial t}=0 \tag{13}$$

$$-h\frac{\partial P}{\partial x}=\frac{\mu}{h}\left(\kappa_x V_x-\kappa_J\frac{U}{2}\right)+\rho h\left\{\frac{\partial V_x}{\partial t}+\frac{\partial V_x^2}{\partial x}+\frac{\partial V_x V_z}{\partial z}\right\} \tag{14}$$

$$-h\frac{\partial P}{\partial z}=\frac{\mu}{h}\kappa_z V_z+\rho h\left\{\frac{\partial V_z}{\partial t}+\frac{\partial V_x V_z}{\partial x}+\frac{\partial V_z^2}{\partial z}\right\} \tag{15}$$

where h is the film thickness, (V_x, V_z) are the buk-flow (film averaged) circumferential and axial flow velocities, P is the pressure, and $(\kappa_x\ \kappa_z)$ denote wall shear stress difference turbulence flow coefficients. These equations are strictly valid for flows without local recirculation zones, i.e. the bulk flow equations are of limited applicability in labyrinth seals or deep groove seals, for example.

Chapters 4 and 5 of Childs textbook [1] provide full descriptions of the analysis and dynamic force response for liquid and gas seals, respectively. San Andrés et al. [11, 12, and 13] extend the model above by including thermal effects and two-phase flow characterization, both effects of importance in cryogenic liquid turbopump applications.

There is commercial software available for prediction of seal leakage and dynamic force coefficients. Most seal practitioners use programs predicting the performance of centered seals, i.e. operating at a null or zero eccentricity. The rationale assumes the seals are NOT load bearing elements. However, this assumption may be quite unrealistic in liquid turbopumps, for example. That is, liquid seals are "load" paths that can affect the load distribution on the support oil lubricated bearings.

The representation of seal forces for lateral motions (X, Y) is

$$\begin{bmatrix}F_X\\F_Y\end{bmatrix}=-\begin{bmatrix}K_{XX}&K_{XY}\\K_{YX}&K_{YY}\end{bmatrix}\begin{Bmatrix}X\\Y\end{Bmatrix}-\begin{bmatrix}C_{XX}&C_{XY}\\C_{YX}&C_{YY}\end{bmatrix}\begin{Bmatrix}\dot{X}\\\dot{Y}\end{Bmatrix}-\begin{bmatrix}M_{XX}&M_{XY}\\M_{YX}&M_{YY}\end{bmatrix}\begin{Bmatrix}\ddot{X}\\\ddot{Y}\end{Bmatrix} \tag{16}$$

where $[K]$, $[C]$, and $[M]$ represent the matrices of stiffness, damping, and inertia force coefficients. Added mass or fluid inertia coefficients are of great importance in liquid seals due to the fluid density and the large flow Reynolds numbers typical of seal flow operation. Recall that fluid inertia effects are not important in (most) mineral oil-lubricated bearings.

Seal analysis at a centered position shows that the direct force coefficients are identical while the cross-coupled coefficients are anti symmetric, i.e. $K_{YY} = K_{XX}$, $K_{XY} = -K_{YX}$, etc.

Note also that the seal force coefficients are frequency independent, i.e. remain constant for changes in excitation or whirl frequency. This assertion is correct only for (nearly) incompressible fluids such as water and liquid oxygen, for example. Other fluids, most

notably gases and liquefied natural gas, are quite compressible. Seals in these applications will produce force coefficients which vary greatly with excitation frequency [3].

San Andrés [8] presents an analysis for fully developed flow through a centered short length annular pressure seal. For small amplitude perturbations in rotor center displacements, a closed form first-order flow field is determined from the linearized fluid flow equations. Close form expressions for the force coefficients due to shaft (rotor) displacements are then derived and compared with predictions from other analyses. The analytical formulation is simple and easy to implement during preliminary pump design stages and multi-variable parametric studies.

A predictive MATHCAD® computational program is available from the author upon request. The software tool is free.

The prediction of annular seal static and dynamic force performance relies on the specification of

- seal geometry (length, diameter and clearance);
- operating conditions, speed and pressure supply and discharge;
- fluid properties (density and viscosity); and,
- empirical coefficients for the inlet pressure loss (ξ) and the inlet swirl ratio (α).

These last parameters are of extreme importance since the direct and cross-coupled stiffnesses depend directly on the seal entrance conditions. At the inlet to the seal section, the typical boundary conditions are

$$P_e = P_s - \frac{1}{2}\rho(1+\xi)V_z^2, \quad V_x = \alpha\,\Omega R \tag{17}$$

where P_e is the fluid entrance pressure at the seal inlet, V_z is the bulk-flow axial velocity, and ξ is a non-isentropic (empirical) entrance loss coefficient. The inlet circumferential speed is a fraction of the rotor speed (ΩR). α=0.50 denotes a 50% inlet swirl typical of an entrance condition into an inter-stage seal or balance piston, for example. $\alpha = \sim 0.60$ is more appropriate at the inlet of a neck-ring seal. As will be seen shortly, the inlet circumferential condition plays a significant role in the generation of cross-coupled stiffness coefficients, the culprit elements leading to rotordynamic instability. In short, an inlet swirl factor α=0.50 leads to a whirl frequency ratio of 50%, i.e. an annular seal is "as bad" as a plain journal bearing in terms of generating follower forces that drive forward whirl in rotating machinery.

Anti-swirl brakes, as shown in Figure 8, are used to reduce the pre-rotation of fluid into the seal, $\alpha \rightarrow 0$. In this way, rotordynamic stability is ensured at the cost of mechanical complexity. Other fixes, in particular in long seals representing balance pistons, include implementing "shunt injection," i.e. forcing liquid somewhere along the seal length in a direction opposite to shaft rotation in order to reduce the development of the circumferential flow speed.

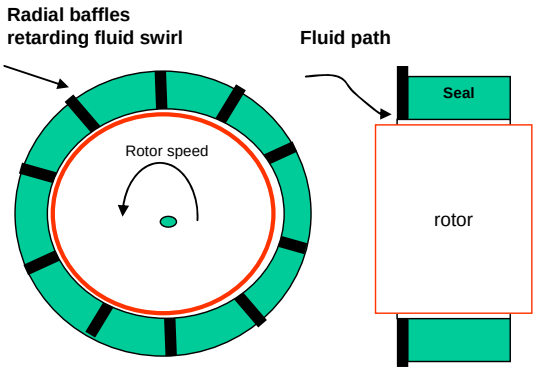

Figure 8: Anti swirl brake at inlet of annular pressure seal

The performance of annular seals is also affected by the condition of the rotor and stator surfaces. Since seals are regarded as rub elements, i.e. subjected to temporary conditions of rubbing at start up and shut down; in practice, predictions are obtained for two clearances, one representing the nominal design or manufactured clearance, and the other clearance at twice the nominal value to denote a worn seal condition in actual operation. These predictions are obtained to determine the effect of clearance on seal leakage rate, power loss and, most importantly, force coefficients affecting the rotor dynamics of the pump (or compressor). In liquid pumps, changes in clearance can affect greatly the direct stiffness thus moving the rotor-bearing system critical speeds (natural frequencies) and producing significant changes in damping ratio.

Comparison of performance between short and long annular seals for a water pump

Predictions of leakage and force coefficients for two water seal configurations representing a neck ring seal (short length, L/D=0.2) and an inter-stage seal (~long seal L/D=0.5) follow. Table 1 shows the geometry of the smooth surfaces seals.

The analysis shows results for the nominal clearance and twice its value representing a worn condition. In addition, an inlet swirl of 50% represents a fluid with an entrance circumferential velocity equal to 50% of rotor surface speed. The swirl factor α=0 denotes the seal with an anti-swirl brake located at the seal inlet. The pressure drop across the seal varies in a quadratic form with rotor speed, $\Delta P \sim \Omega^2$, with the nominal condition noted in the table. The speed range for the predictions is 1,000 to 5,000 rpm.

Table 1: geometry and operating conditions of water seals in a liquid pump

D = 152. 4 mm, L/D=0.20 and 0.50
c=0.190 mm, nominal clearance
smooth rotor and stator surfaces
Nominal speed = 3600 rpm and pressure drop 34.4 bar
Inlet loss coefficient ξ=0.1, Inlet swirl α=0.5 and 0.0
Fluid: water at 30°C (0.792 cPoise, 995 kg/m^3)

In the following figures, the left graphs show predictions for the long seal (*L/D*=0.50); while on the right graphs, results are depicted for the short seal, *L/D*=0.20. In addition, the predictions are shown are for the condition of inlet swirl at 50% rotor speed, unless otherwise stated. That is, the change in inlet swirl does not affect significantly several of the seal flow performance parameters. When important, the graphs and discussion will focus on this aspect.

Inlet pressure. Figure 9 depicts the supply pressure into the seal increasing with rotor speed. The entrance pressures are lower for the worn seal (2*c)* due to an increase in flow rate that magnifies the fluid inertia inlet effect. The short seal shows a larger entrance pressure drop since the flow rate across the seal is larger (larger axial flow velocity). Inlet swirl has a minimal effect on the entrance pressure into the seal.

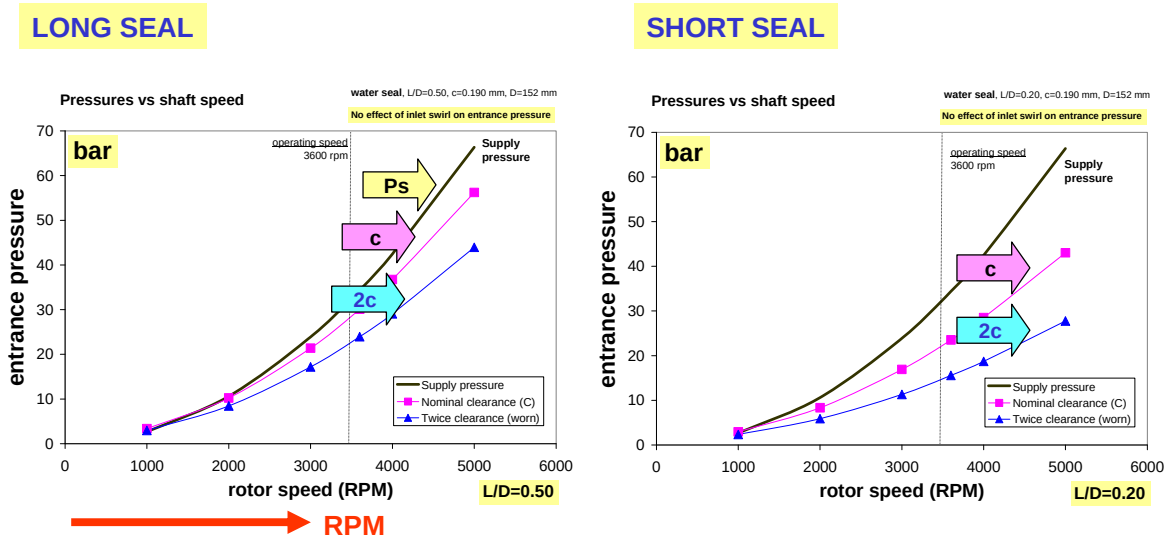

Figure 9: Supply and entrance pressures for two water seals, *L/D*=0.50 and 0.20, and two clearances (*c* and 2*c*) versus rotor speed

Flow rate. Figure 10 shows the worn seals (enlarged clearances) leak more than at the nominal clearance condition. The short length seals have a larger flow rate in spite of the reduced entrance pressure. The penalty in leakage increase as the seal wears will affect the overall efficiency of the liquid pump. Inlet swirl has no discernible effect on seal leakage. The seal leakage appears as proportional to shaft speed. However, its variation is proportional to $\Delta P^{1/2}$. Recall that the pressure drop varies with rotor speed, Ω^2.

Drag Power. Figure 11 shows that the long seals (*L/D*=0.5) have a larger drag power (torque x rotational speed) than the short length seals due to the larger area of fluid flow shearing. Inlet swirl is not significant in spite that the mean flow circumferential speed may be much less than 50% of rotor surface speed.

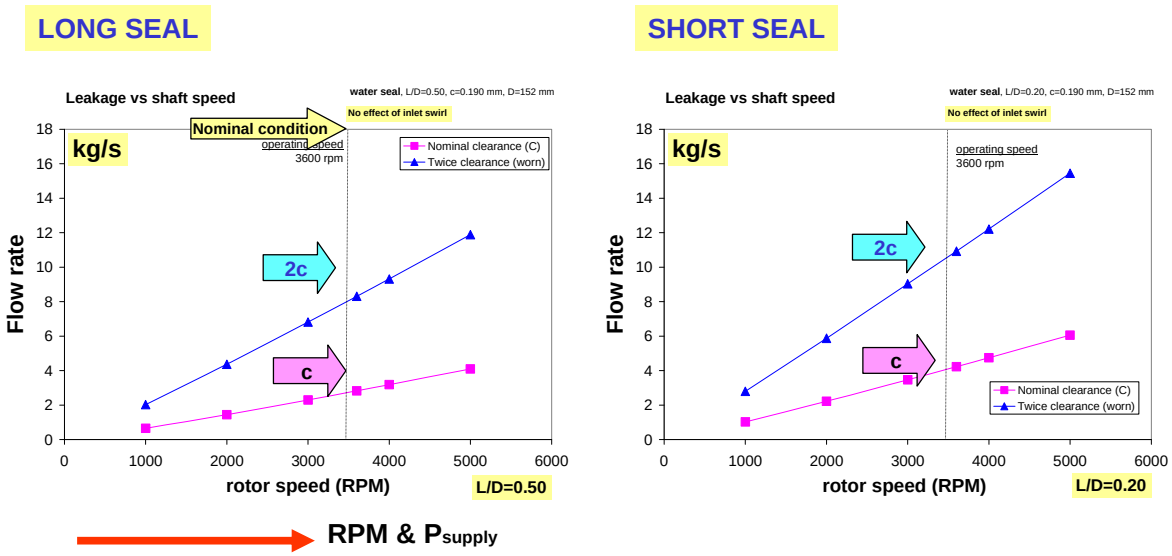

Figure 10: Leakage (flow rate) for two water seals, *L/D*=0.50 and 0.20, and two clearances (*c* and 2*c*) versus rotor speed

Direct stiffness. Figure 12 depicts the direct stiffness coefficients, K_{XX}=K_{YY}, increasing rapidly with rotor speed, i.e. with supply (or entrance) pressure. The direct stiffness for the long seal is about twice as large as for the short seal, and comparable in magnitude to the stiffnesses of any oil lubricated bearing, for example. The worn seals show a dramatic reduction in direct stiffness. For example, at the nominal operating condition of 3,600 rpm, the direct stiffnesses are ~50% of the values for the nominal clearances. This stiffness reduction will affect considerably the rotordynamic behaviour of a liquid pump. Recall that "wet" critical speeds depend on the seal direct stiffnesses which clearly drop as the seal wears out.

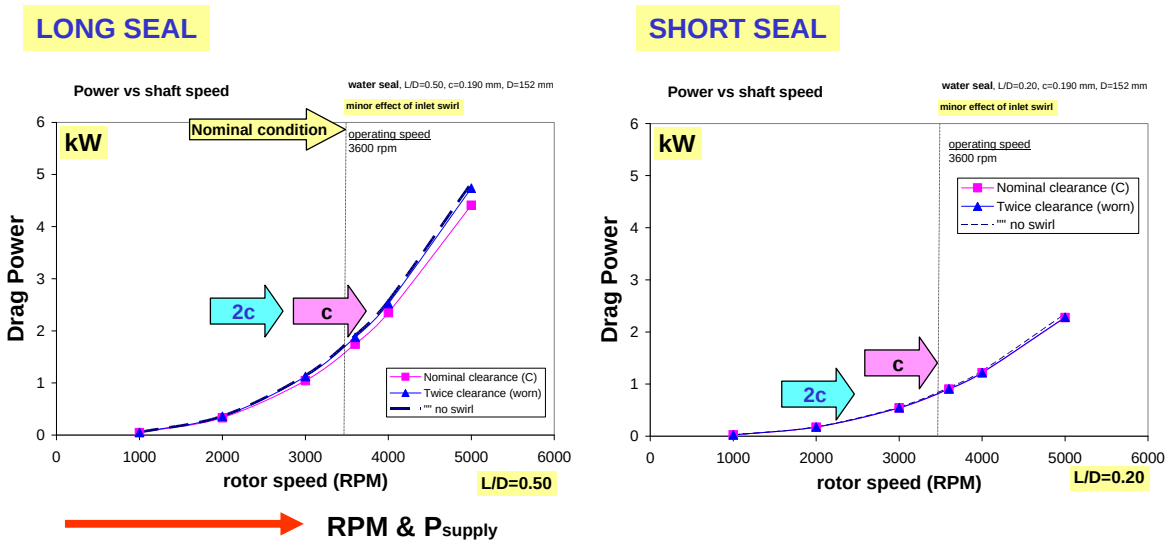

Figure 11: Drag power for two water seals, *L/D*=0.50 and 0.20, and two learances (*c* and 2*c*) versus rotor speed

Cross-coupled stiffness. Figure 13 displays the cross-coupled stiffness coefficients, $K_{XY} = -K_{YX}$, also increasing rapidly with rotor speed. The operating clearance has a direct impact on the generation of cross-coupled forces, in general $K_{XY} \sim 1/c$ for turbulent flow seals. Note that the vertical scale in both graphs is different. The long seal shows about five times larger cross-coupled stiffness than the short seal's. The impact of inlet swirl is profound in the generation of cross-coupled forces. Note that in the long seal, a null pre swirl, α=0.0, aids to reduce considerably the generation of K_{XY} since the circumferential flow is greatly retarded. This effect is more pronounced for the worn seal since the increase in leakage pushes faster the fluid through the seal without it having enough time to evolve towards the 50% surface speed condition.

In the short length seal, on the other hand, the effect of null pre swirl is remarkable. The cross-coupled coefficients are effectively null (zero magnitude). Note that $K_{XY} < 0$ denotes a most favorable condition to avoid synchronous forward whirl, i.e. the cross-coupled stiffness force acts effectively as a damping force.

At the nominal operating condition, for the long seal and with a pre swirl ratio of 50%, K_{XY} is as large as the direct stiffness coefficient, K_{XX}, see Figure 12. In the short length seal, K_{XY} 's are not as large as the direct stiffnesses. The larger the cross-coupled coefficients, the smaller the effective damping acting on the rotor-bearing system, $C_{ef} = C_{XX} - (1/\omega)K_{XY}$.

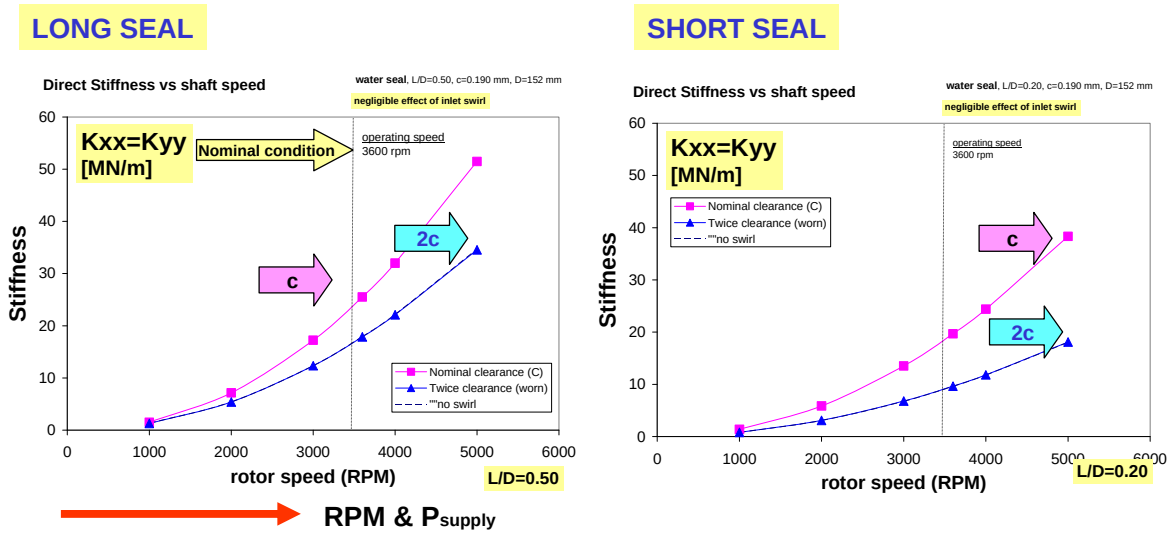

Figure 12: Direct stiffness coefficients for two water seals, *L/D*=0.50 and 0.20, and two clearances (*c* and 2*c*) versus rotor speed

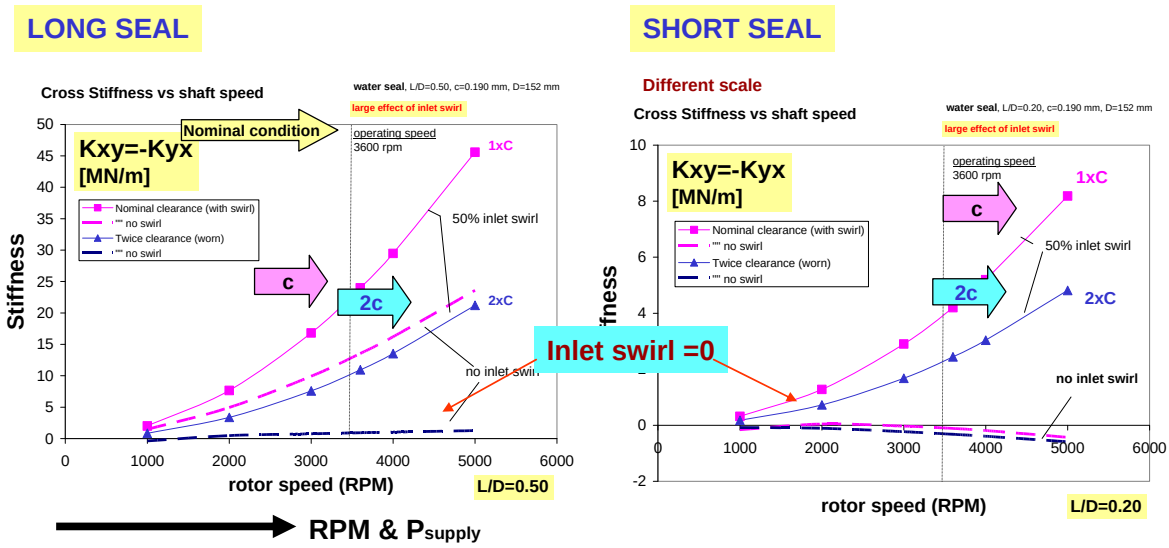

Figure 13: Cross-coupled stiffness coefficients for two water seals, *L/D*=0.50 and 0.20, and two clearances (*c* and 2*c*) versus rotor speed (note difference in vertical scales)

Damping coefficients. Figure 15 shows the direct (C_{XX}=C_{YY}) and cross-coupled damping (C_{XY}=-C_{YX}) coefficients for the two seals. In general, $C_{XY} < C_{XX}$, except for seals handling compressible fluids (gases). Incidentally, inlet pre swirl, α=0.0-0.50, has a negligible effect on the generation of damping coefficients. Damping arises from squeeze film effects and is not directly a function of rotor speed. The damping coefficients are a function of the effective turbulent flow viscosity, a function of the flow Reynolds number which increases with the pressure drop across the seal. In addition, for turbulent flows, the direct damping is inversely proportional to the operating clearance[2]. Note that the vertical scales in both graphs are different. Thus, the long seal shows about five times larger direct damping than the short length seal. Seal wear enlarging its operating clearance leads to a dramatic drop in direct damping.

[2] In laminar flow journal bearings, the damping and cross-stiffness coefficients are proportional to $(1/c)^3$. See Lecture 5. That is, they grow rapidly with a decrease in clearance (c).

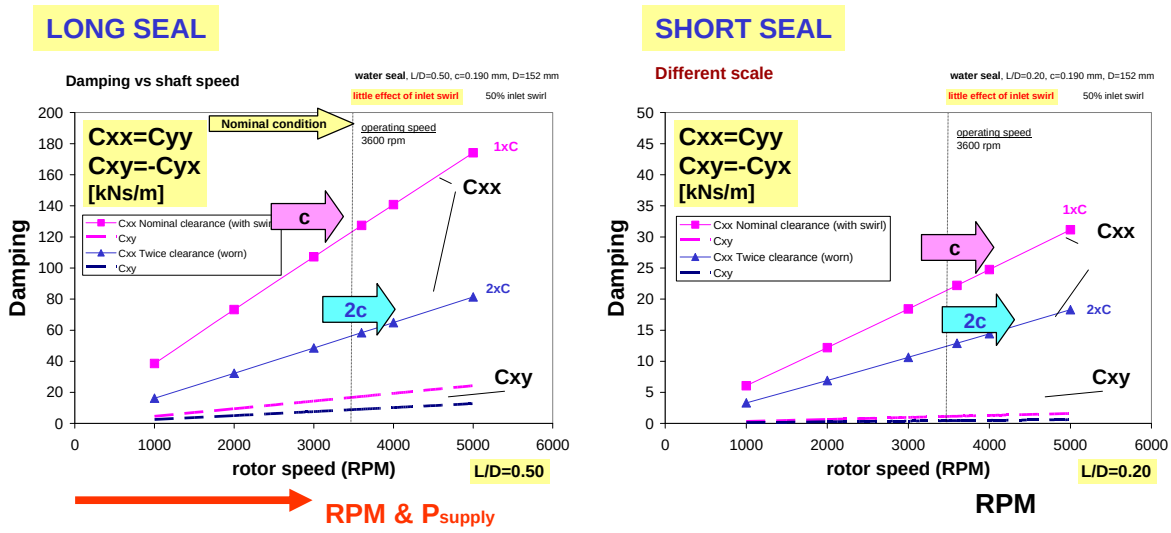

Figure 14: Direct and cross-damping coefficients for two water seals, *L/D*=0.50 and 0.20, and two clearances (*c* and 2*c*) versus rotor speed (note difference in vertical scales)

Inertia force coefficients. Figure 15 shows the direct (M_{XX}=M_{YY}) added mass coefficient for the two seals. In general, $|M_{XY}| < M_{XX}$, and thus not shown here. Inlet swirl has no discernible effect on the direct inertia force coefficient. Note that the added mass is practically invariant with shaft speed, in particular for the long seal case. Incidentally, note the different scales in both graphs. The long seal renders a much larger inertia coefficient. Its magnitude is significant and will be added as an apparent mass into the pump rotor dynamic structural model. This is one more reason for the differences between "wet" and "dry" critical speeds in liquid pumps.

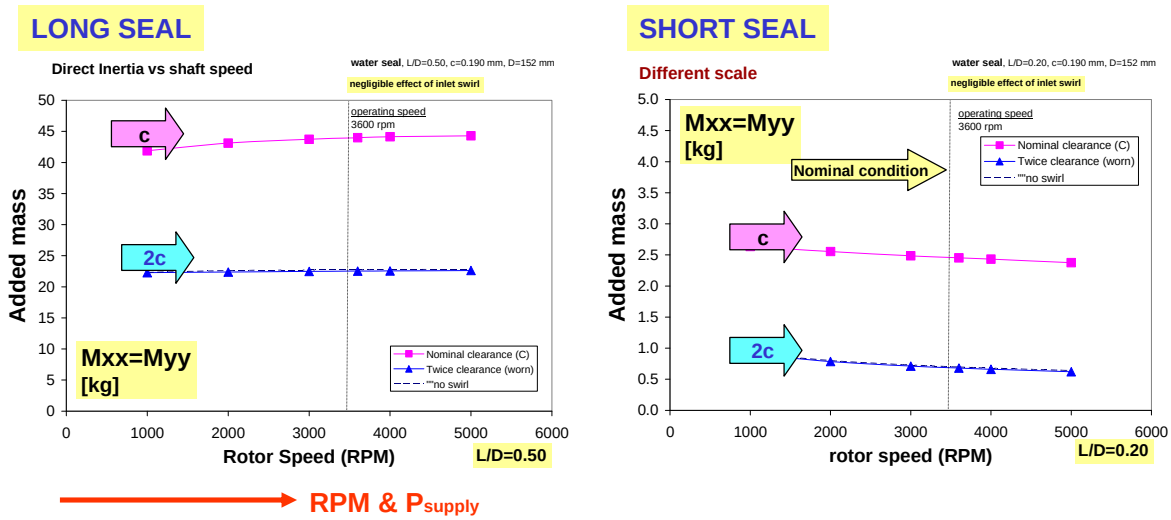

Figure 15: Direct and cross-inertia force coefficients for two water seals, *L/D*=0.50 and 0.20, and two clearances (*c* and 2*c*) versus rotor speed (note differences in vertical scale)

The equation below gives a closed form expression for prediction of the added mass coefficient (M_{XX}) in a seal or squeeze film damper [14]. The simple formula will serve to realize the importance of fluid inertia on seal dynamic force performance. M_{fluid} denotes the mass of liquid within the seal film land while M_{steel} represents the mass of a solid piece of steel with density set to 7,800 kg/m^3.

$$M_{fluid} := \rho \cdot \pi \cdot D \cdot L \cdot c \qquad M_{steel} := \rho_{steel} \cdot \pi \cdot \left(\frac{D}{2}\right)^2 \cdot L$$

$$M_{XX} := \rho \cdot \pi \cdot \left(\frac{D}{2}\right)^3 \cdot \frac{L}{c} \cdot \left(1 - \frac{\tanh\left(\frac{L}{D}\right)}{\frac{L}{D}}\right) \qquad (18)$$

The calculated magnitudes of added mass coefficients for the short and long seals (nominal clearance) are

$\frac{L}{D} = 0.2$ $\quad M_{XX} = 2.91\text{kg}$ $\quad M_{fluid} = 2.76 \times 10^{-3}\,\text{kg}$ $\quad M_{steel} = 4.34\text{kg}$ $\quad \frac{M_{XX}}{M_{steel}} = 0.67$

$\frac{L}{D} = 0.5$ $\quad M_{XX} = 42.03\text{kg}$ $\quad M_{fluid} = 6.9 \times 10^{-3}\,\text{kg}$ $\quad M_{steel} = 10.84\text{kg}$ $\quad \frac{M_{XX}}{M_{steel}} = 3.88$

Although the mass of water contained within the seal land is just a few grams, the seal added mass coefficient is orders of magnitude larger. The added mass or inertia coefficient (M_{XX}) is of the same order of magnitude, and for L/D=0.5 even larger, than the mass of a solid piece of rotor of identical length. The approximate formula is very good for quick estimations of added mass coefficients, as a direct comparison to the numerical results shown in Figure 15 attests.

Recently, Delgado [15] develops a comprehensible analysis for the prediction of damping and added mass coefficients in seals and dampers with internal grooves. The author demonstrates that both feed and inner-land grooves in annular seals act to amplify significantly the seal added mass, predicted magnitudes are much larger than simple models would otherwise predict, e.g. Eqn. (18). The novel analysis is on the mark when reproducing unusual test results obtained by Childs et al. [16].

Whirl frequency ratio: Figure 16 depicts the stability indicator (*WFR*) for the two seals. With an inlet pre-swirl equal to 50% of rotor speed, the *WFR* is always 0.50. In this case, $K_{XY}/(\Omega\, C_{XX})$ =0.50, indicates that the pump can not operate at a sped above twice the critical speed of the rotor-bearing-seal system. Furthermore, consider that this critical

speed is the "wet" one, i.e. lower than the "dry" critical speed, since fluid inertia effects will effectively reduce the "dry" system natural frequency.

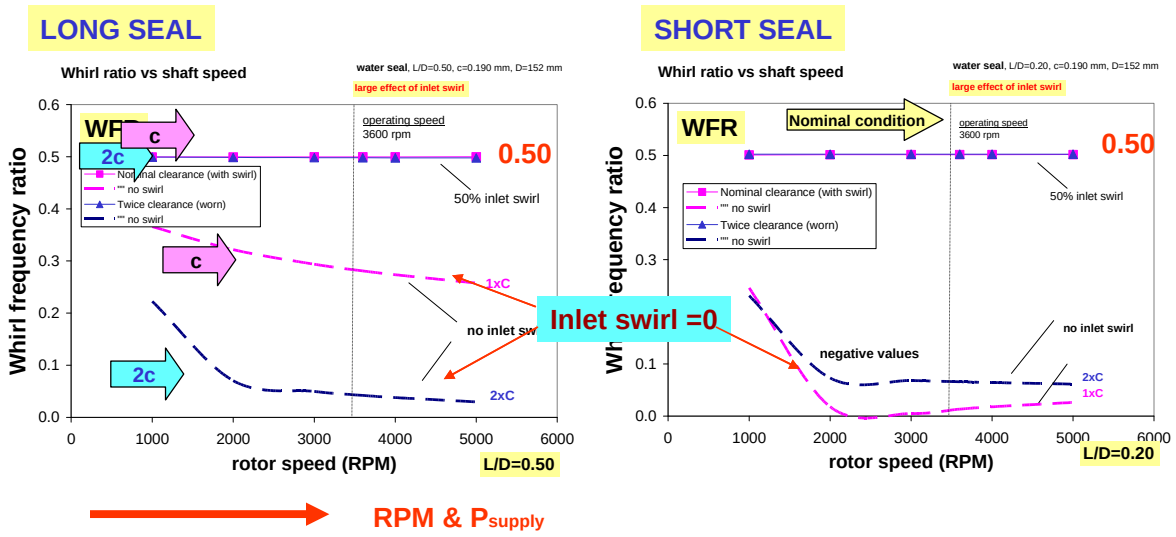

Figure 16: Whirl frequency ratio for two water seals, *L/D*=0.50 and 0.20, and two clearances (*c* and 2*c*) versus rotor speed (note difference in vertical scales)

The effect of an anti-swirl break on the performance of the seal is dramatic. For a condition of no pre-swirl, the short length seal actually presents a negative whirl frequency ratio, meaning that the seal is impervious to (unstable) forward rotor whirl motions. The effect of the null pre-swirl is less notorious in the long seal, since the fluid flowing through the seal does have enough "residence" time to develop a circumferential mean flow velocity approaching the 50% rotor speed. Clearly, swirl brakes are inefficient devices for very long seals, $L/D > 1$, as it would be the case of a balance piston, for example.

Extensive experimentation demonstrated that seals with macroscopic roughness; i.e. **textured stator surfaces**, offer major improvements in reducing leakage as well as cross-coupled stiffness coefficients [2]. Figure 17 depicts two textured seals and a conventional labyrinth seal (teeth on stator). A textured surface like a round-hole pattern or a honeycomb increases the friction thus reducing leakage, and aids to retard the development of the circumferential flow velocity -the physical condition generating the cross-coupled stiffness coefficients. However, surface texturing on the rotor works the other way around while still reducing leakage, i.e. the circumferential flow develops faster causing even more severe rotordynamic instabilities. Since the late 1990s, compressor and pump manufacturers, as well as end users, are implementing efficiently textured seals with great commercial success [17].

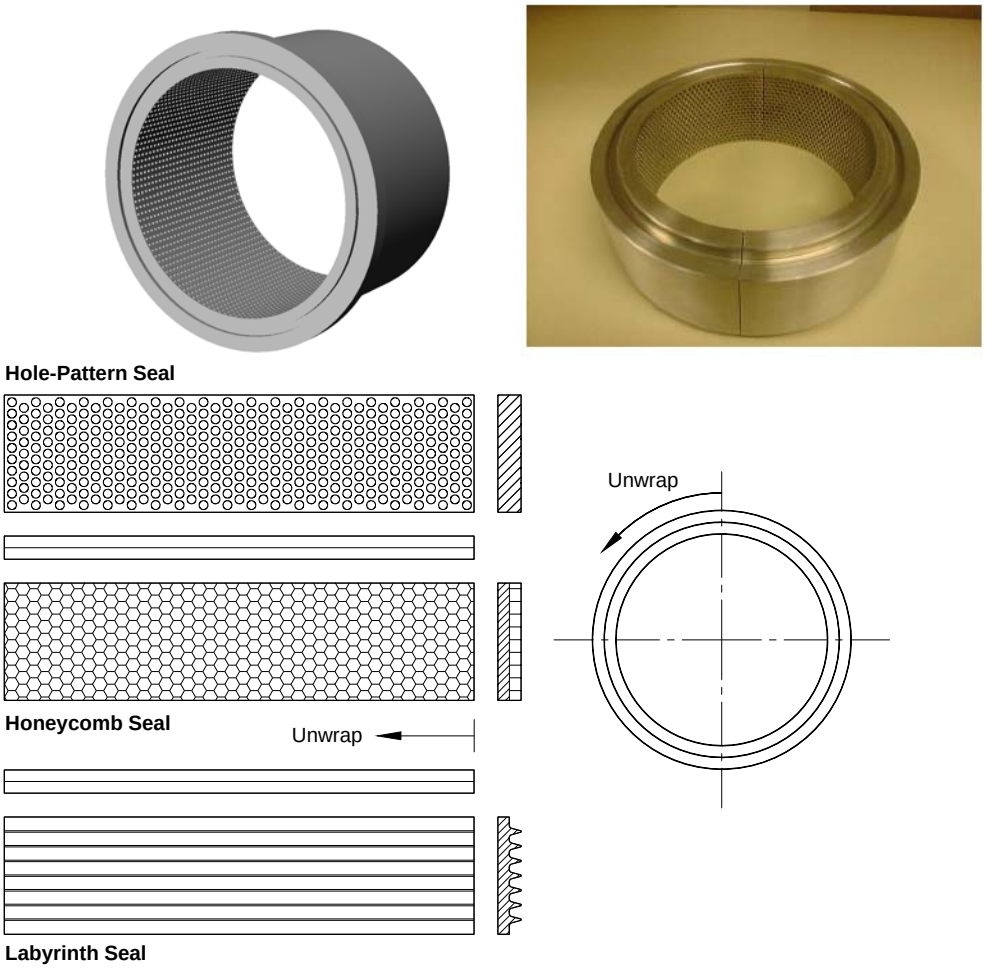

Figure 17: Hole-pattern, honeycomb and labyrinth seal configurations

References

[1] Turbomachinery Rotordynamics, (chapter 4), D. Childs, John Wiley & Sons, Inc., 1993.

[2] Damping Seals for Turbomachinery, G. von Pragenau, NASA Technical Paper No. 1987, 1982.

[3] Annular Gas Seals and Rotordynamics of Compressors and Turbines, D. Childs & J. Vance, Proc. Of the 26th Turbomachinery Symposium, TAMU, pp. 201-220, 1997.

[4] Pump Rotordynamics made Simple, M. Carbo & S. Malanoski, Proc. Of the 15th International Pump Users Symposium, TAMU, pp. 167-203, 1998.

[5] Effects of Hydraulic Forces on Annular Pressure Seals on the Vibrations of Centrifugal Pump Rotors, H. Black, Journal of Mechanical Engineering Science, **11**(2), pp. 206-213.

[6] Analysis of Variable Fluid Properties, Turbulent Annular Seals, L. San Andrés, ASME Journal of Tribology, **113**, pp. 694-702, 1991.

[7] Advances in Mechanical Sealing – An Introduction to API 682 Second Edition, M. Huebner, J. Thorp, C. Buck & C. Fernandez, Proc. Of the 19th International Pump Users Symposium, TAMU, 2004.

[8] Introduction to Annular Pressure (Damper) Seals, L. San Andrés, Lecture Notes (#11) in Modern Lubrication, http://phn.tamu.edu/TRIBGroup, 2002.

[9] A Bulk-Flow Theory for Turbulence in Lubricant Films, G.G. Hirs, ASME Journal of Lubrication Technology, **94**, pp. 137-146. 1973.

[10] Effect of Shaft Misalignment on the Dynamic Force Response of Annular Pressure Seals, L. San Andrés, STLE Tribology Transactions, **36**, 2, pp. 173-182, 1993

[11] Thermal Effects in Cryogenic Liquid Annular Seals, I: Theory and Approximate Solutions, L. San Andrés, Z. Yang & D. Childs, ASME Journal of Tribology, **115**, 2, pp. 267-276, 1993.

[12] Thermal Effects in Cryogenic Liquid Annular Seals, II: Numerical Solution and Results, Z. Yang, L. San Andrés & D. Childs, ASME Journal of Tribology, **115**, 2, pp.277-284, 1993.

[13] Analysis of Two Phase Flow in Cryogenic Damper Seals, I: Theoretical Model, II: Model Validation and Predictions, G. Arauz & L. San Andrés, "ASME Journal of Tribology, **120,** pp. 221-233, 1998.

[14] Squeeze Film Dampers: Operation, Models and Technical Issues, L. San Andrés, Lecture Notes (#13) in Modern Lubrication, http://phn.tamu.edu/me626, 2009.

[15] A. Delgado, A Linear Fluid Inertia Model for Improved Prediction of Force Coefficients in Grooved Squeeze Film Dampers and Grooved Oil Seal Rings, (2008), Ph.D. Dissertation, Texas A&M University, College Station, TX.

[16] D. W. Childs, M. Graviss and L.E. Rodriguez, The Influence of Groove Size on the Static and Rotordynamic Characteristics of Short, Laminar-Flow Annular Seals, ASME J. Tribol, (2007), 129(2), 398-406.

[17] Gas Damper Seal Test Results, Theoretical Correlation, and Applications in Design of High-Pressure Compressors, P. De Choudhury, F. Kushner & J. Li, Proc. Of the 29th Turbomachinery Symposium, TAMU, 2001.

Visit URL http://rotorlab.tamu.edu to learn more about research in annular gas seals sponsored by industry. Recent work in high temperature gas labyrinth seals and brush seals for power gas turbines is showcased. The site displays existing test rigs, experimental data, and comparisons to model predictions. The site also provides a full list of technical reports and archival papers on annular seals, oil seals and hybrid brush seals.